Proceedings of the XII Serbian-Bulgarian Astronomical Conference (XII SBAC) Sokobanja, Serbia, September 25-29, 2020
Editors: L. Č. Popović, V. A. Srećković, M. S. Dimitrijević and A. Kovačević
Publ. Astron. Soc. "Rudjer Bošković" No 20, 2020, 43-49

EVOLUTION OF MASSIVE BINARY SYSTEMS: PRIMARY STAR EVOLUTION INTO A NEUTRON STAR

JELENA PETROVIC

Astronomical Observatory, Volgina 7, 11000 Belgrade, Serbia
E-mail: jpetrovic@aob.rs

Abstract. The sources of gravitational waves, observed by the LIGO and Virgo detectors, have been linked with mergers in binary systems (Abbott et al. 2019). Those systems are consisting of compact objects - black holes and/or neutron stars. Progenitors of those systems are massive binary systems and initial masses of above ~30 $M_{\odot}$ are needed for the formation of double black holes. We present examples of evolutionary models of massive binary systems with initial masses around 30 $M_{\odot}$ and we follow their evolution until the primary stars form an iron core. The initial orbital period is set at 3 days and the initial mass ratio is 0.9. Those models are calculated with the MESA (Modules for Experiments in Stellar Astrophysics) stellar evolution numerical code. We find that primary stars in those systems evolve into neutron stars.

1. INTRODUCTION

Recent discovery of gravitational waves by the LIGO and Virgo collaborations (Abott et al. 2019) has linked those events with mergers in double compact binary systems, consisting of neutron stars and/or black holes, the end products of stellar evolution in massive close binary systems. Initial masses of above ~30 $M_{\odot}$ are shown to be necessary to produce black hole relics (Kruckow et al. 2018).

The primary star in a binary system, the component with the greater mass, evolves faster than the secondary and through envelope expansion may reach the radius of its Roche lobe and starts transferring mass onto the secondary star. This process is called Roche Lobe Overflow (RLOF). A star in a binary can reach its Roche lobe radius during different phases of evolution: core hydrogen burning, shell hydrogen burning or after the onset of central helium burning, corresponding respectively to Case A, B and C of mass transfer. However, in case there is a mass transfer during the core hydrogen burning – Case A, mass transfer during the shell hydrogen burning phase is called Case AB. Case ABB is then the third mass transfer that takes place after helium core burning is completed.

Evolutionary models of massive binary stars, evolving via the stable mass transfer channel and considering different accretion efficiencies, have been presented by many authors (for example De Greve and De Loore 1992, Pols 1994, De Loore and Vanbeveren 1994, Wellstein and Langer 1999, Wellstein et al. 2001, Petrovic et al. 2005). Wellstein et al. (2001) have shown that the initial mass ratio in massive binaries should be near unity, otherwise the system evolves into a contact, or in other words, the secondary star expands due to accretion and both stars fill their Roche lobes. Petrovic et al. (2005) have modeled progenitor evolution of observed Wolf Rayet + O binary systems an they found that the most likely evolution is via Case A mass transfer with accretion efficiency of only 10%.

Double compact objects are relics of massive binary star evolution.

Such binary systems start as double O-type stars and evolve through multiple interactions in their lifetimes, transferring matter and angular momentum from one to another. Those systems evolve through a Wolf-Rayet + O phase and survive two supernova explosions. The orbits of massive close binaries are most probably tidally circularized and eccentricity is not an important parameter to consider (Hurley 2002).

In this paper, we present the calculations of the evolution of the initial binary systems: 30 + 27 $M_\odot$ and 32 + 28.8 $M_\odot$, both with initial orbital period of 3 days and initial mass ratio of 0.9. We follow the evolution of the primary star through three Roche lobe overflows (Case A, AB and ABB) until iron core formation.

2. MODELS

For the calculation of the evolution of binary models presented in this paper, the MESA (Modules for Experiments in Stellar Astrophysics) code was used (Paxton et al. 2011, 2013, 2015, 2018). Models with initial masses 30 + 27 $M_\odot$ and 32 + 28.8 $M_\odot$, both with initial orbital period of 3 days and initial mass ratio of 0.9 are presented. Metallicity is set to 0.02.

The MESA code calculates simultaneously the evolution of both stars within a binary system. Mass transfer happens via the L_1 Lagrangian point and its rate is calculated according to the Ritter scheme (Ritter 1988). The composition of accreted material is identical to the donor's current surface composition. It is assumed that the mass lost in the stellar wind has the specific orbital angular momentum of its star. For the case of inefficient mass transfer, angular momentum loss follows Soberman et al. (1997) where fixed fractions of the transferred mass are lost as a fast isotropic wind. Stellar wind mass loss is calculated according to Vink et al. (2001).

3. RESULTS AND DISCUSSION

The modeled binaries start their evolution as detached systems with an orbital period of 3 days and evolve through three mass transfers. We follow the evolution of the binary systems until iron core formation in the primary stars.

The primary stars in both binary systems (30 + 27 M⊙ and 32 + 28.8 M⊙) fill their Roche lobe first time during the core hydrogen burning phase. At this time they still have about 30% of hydrogen left in their cores. During Case A mass transfer, the primary stars lose a significant amount of their mass (about 15 M⊙). The secondary stars accrete only 10% of the mass lost by the primaries, and due to the high stellar wind mass loss, they actually slightly decrease their initial masses. After the core hydrogen burning phase, the primary stars expand, mass transfer starts again and lasts until the primary stars ignite helium in their cores. Finally, after the core helium burning phase, there is one more expansion of the primary star that leads to Roche lobe overflow.

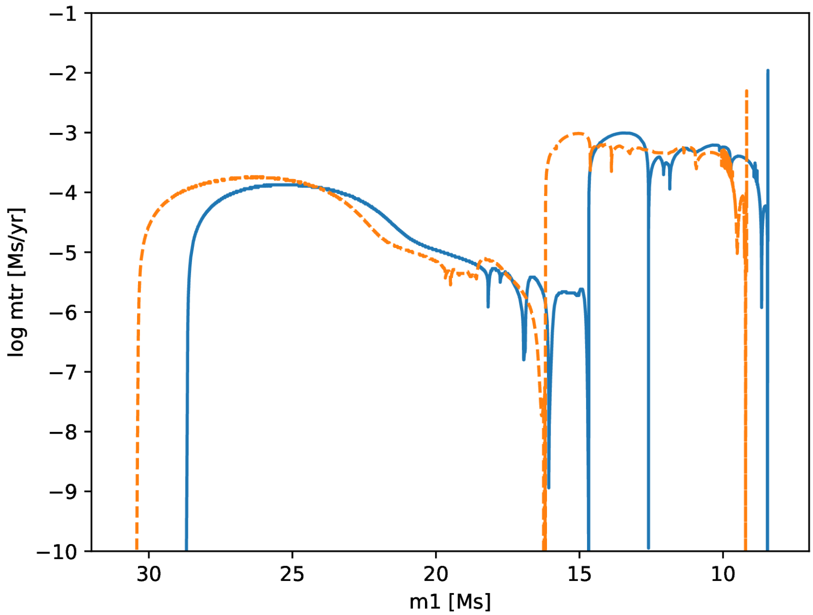

Figure 1: Mass transfer rate as a function of the primary mass in binary systems 30 + 27 M⊙ (blue solid line) and 32 + 28.8 M⊙ (orange dashed line), both with initial orbital period of 3 days and accretion efficiency of 10%.

Figure 1 shows the mass transfer rate in modeled systems as a function of the primary mass. The first mass transfer (Case A) starts when the primary stars are 28.8 and 30.5 $M_\odot$, slightly less massive than initially due to the stellar wind mass loss. After Case A mass transfer, the primary masses are 14.7 and 16.2 $M_\odot$. The corresponding secondary masses are 26.9 and 28.4 $M_\odot$. When the core helium burning phase starts, the primary masses are 8.4 and 9.2 $M_\odot$ and the secondary masses are 27.4 and 29.0 $M_\odot$.

The mass transfer rate during Case A in both systems is in the order of magnitude of 10^{-4} $M_\odot$/yr in its maximum. During the following mass transfer, it reaches a value one order of magnitude higher. The last peak on this plot represents the beginning of the last mass transfer. At the same time, an iron core is formed in the primary stars.

During the evolution from the main sequence to the formation of the iron core, the orbital period increases from the initial 3 days to 7.7 and 7.6 days during Case A mass transfer and to 27.1 and 26.8 days during the subsequent mass transfer.

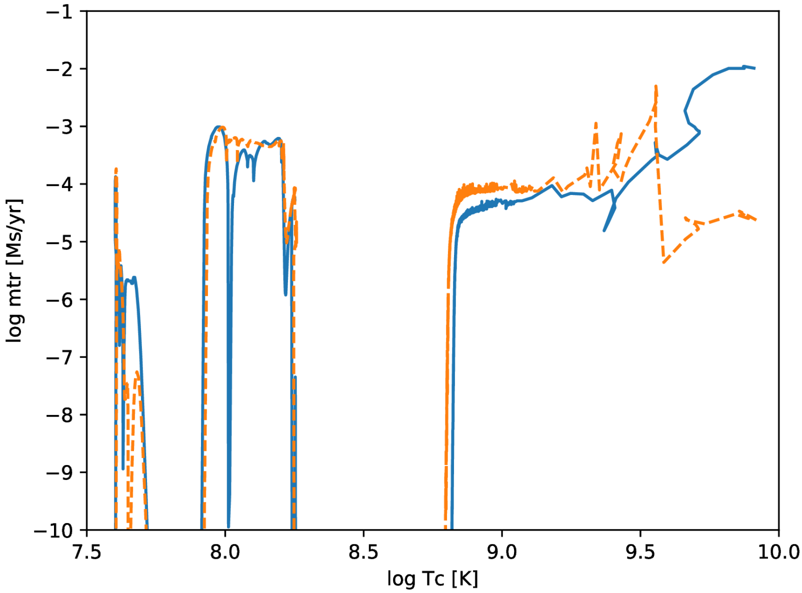

Figure 2: Mass transfer rate as a function of the primary star central temperature in binary systems 30 + 27 $M_\odot$ (blue solid line) and 32 + 28.8 $M_\odot$ (orange dashed line), both with initial orbital period of 3 days and accretion efficiency of 10%.

Figure 2 also shows mass transfer rate, but as a function of the central temperature of the primary star. Here we can clearly see three mass transfer phases for both systems. The last mass transfer starts after helium core burning is completed and it corresponds with a fast increase of the central temperature accompanied by the formation of a carbon, oxygen, silicon and iron core in the primary stars in the modeled systems.

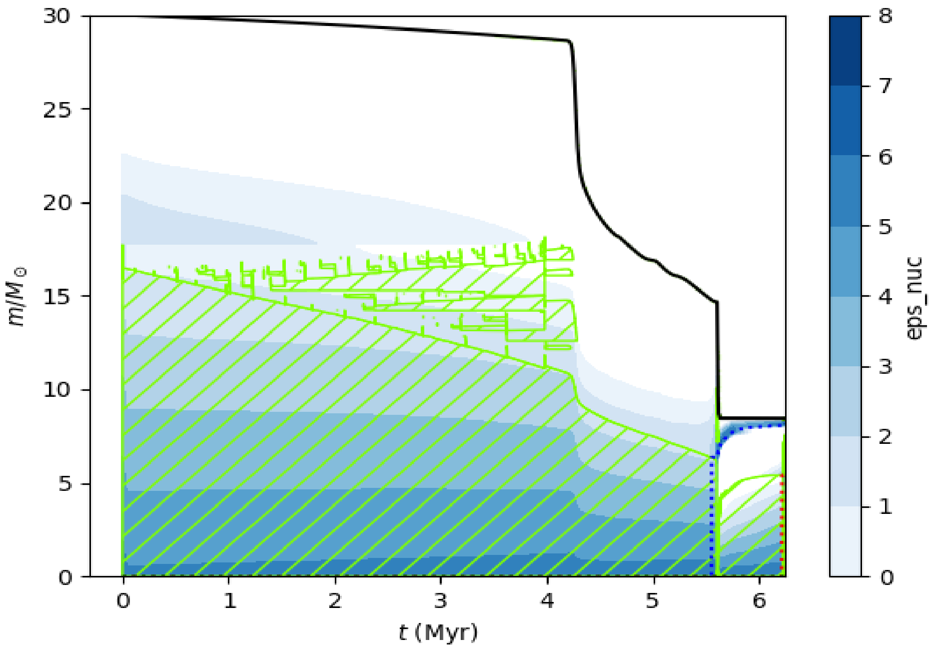

Figure 3: Convective plot of the primary star in binary system 30 + 27 M⊙ for initial orbital period of 3 days and accretion efficiency of 10%. X-axis shows time and y-axis shows stellar mass. Top black line presents the mass of the primary. Blue regions mark nuclear burning zones, darker shades indicate large intensity. Green diagonally hatched areas indicate convection zones. Blue dotted line presents mass of helium core and red dotted line mass of carbon-oxygen core.

Figure 3 shows a so-called Kippenhahn plot of the internal structure evolution of the primary star in the system 30 + 27 M⊙. The top black line presents the mass of the primary. At the age of about 4 million years and 5.6 million years, large mass loss due to mass transfers is visible. The helium core is formed at about 5.6 million yeas and its mass is 8.14 M⊙, the carbon-oxygen core is formed at about 6.2 million years with a mass of 5.41 M⊙.

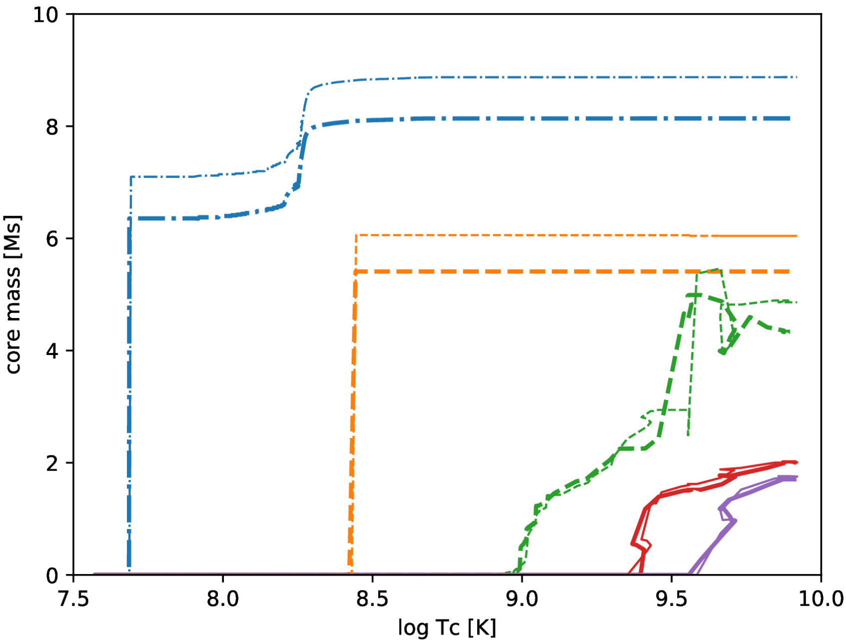

Figure 4: Core masses as a function of central temperature for primary stars in binary systems 30 + 27 M⊙ (thick lines) and 32 + 28.8 M⊙ (thin lines) with initial period of 3 days and accretion efficiency of 10%. Helium core mass is presented with a blue line, carbon with orange, oxygen with green, silicon with red and iron with a purple line.

In binary system 32 + 28.8 M⊙, the masses of the helium and CO cores are slightly larger due to the larger initial mass of the primary. Figure 4 shows helium, carbon, oxygen, silicon and iron core masses as a function of central temperature in primary stars for both binary systems. The mass of the helium and carbon-oxygen core in binary system 32 + 28.8 M⊙ are 8.87 and 6.04 M⊙ respectively. Both presented primary stars have a final carbon-oxygen core less massive than 6.5 M⊙, which indicates that they evolve into neutron stars after an iron-core collapsing supernova explosion (Kruckow et al. 2018, Tauris et al. 2015).

4. CONCLUSIONS

In this paper, we present evolutionary paths of primary stars in two massive binary systems: 30 + 27 M⊙ and 32 + 28.8 M⊙ with initial orbital period of 3 days and accretion efficiency of 10%. Initial parameters and accretion efficiency value are selected based on the progenitor models of Wolf-Rayet + O observed binary systems by Petrovic at al. (2005) and evolutionary models by Wellstein et al. (2001).

The presented calculations follow the evolution of two massive binary systems until the primary forms an iron core. Subsequently, the primary will explode as a supernova and leave a neutron star as a relic (CO core mass < 6.5 $M_\odot$). If the binary system remains bound after this SN explosion (type Ib/c), it will eventually be observable as a high-mass X-ray binary (HMXB).

After some time, the secondary star expands enough to fill its Roche lobe and starts transferring mass onto the neutron star. The system may become dynamically unstable and enter the so-called common envelope (CE) phase. In this phase, dynamical friction of a neutron star inside an envelope of a secondary star results in a large orbital momentum loss and a decrease in orbital period. Eventually, the secondary star also explodes as a supernova, leaving a compact object as a relic.

In the cases of the calculated systems, at the time of the supernova explosions of the primary stars, secondaries, that are still core hydrogen burning stars, have masses of about 27 and 29 $M_\odot$. Those masses indicate that the presented systems likely evolve into double neutron stars. If their orbital periods stay relatively short after the second supernova explosion, such double compact binary systems eventually merge and give rise to powerful emission of gravitational waves.

References

Abbott B. P. et al. (LIGO Scientific Collaboration and Virgo Collaboration): 2019, *Phys. Rev. X*, 9, 031040.
De Greve J. P., De Loore C.: 1992, *A&AS*, 96, 653.
De Loore C., Vanbeveren D.: 1994, *A&A*, 292, 463.
Hurley J. R., Tout, C. A., Pols O. R.: 2002, *MNRAS*, 329, 897
Kruckow M. U., Tauris M. T., Langer N. et al.: 2018, *MNRAS,* 481, 1098.
Paxton B., Bildsten L., Dotter A. et al.: 2011, *ApJS*, 192, 3.
Paxton B., Cantiello M., Arras P. et al.: 2013, *ApJS*, 208, 4.
Paxton B., Marchant P., Schwab J. et al.: 2015, *ApJS*, 220, 15.
Paxton B., Schwab J., Bauer E. B. et al.: 2018, *ApJS*, 234, 34.
Petrovic J., Langer N., van der Hucht K.: 2005, *A&A*, 435, 1013.
Pols O.: 1994, *A&A*, 290,119.
Ritter H.: 1988, *A&A*, 202, 93.
Soberman G. E., Phinney E. S., van den Heuvel E. P. J.: 1997, *A&A*, 327, 620.
Vink J.S., de Koter, A. Lamers H. J. G. L. M.: 2001, *A&A*, 369, 574.
Tauris T. M., Langer N., Podsiadlowski P.: 2015, *MNRAS*, 451, 2123.
Wellstein S., Langer N.: 1999, *A&A*, 350, 148.
Wellstein S., Langer N., Braun H.: 2001, *A&A*, 369, 939.